remote sensing

MDPI

Article

Determining Optimal New Generation Satellite Derived Metrics for Accurate C3 and C4 Grass Species Aboveground Biomass Estimation in South Africa

Cletah Shoko [1,*], Onisimo Mutanga [1] and Timothy Dube [2]

[1] Discipline of Geography, School of Agricultural, Earth and Environmental Sciences, University of KwaZulu-Natal, Private Bag X01, Scottsville, Pietermaritzburg 3209, South Africa; mutangaO@ukzn.ac.za
[2] Department of Earth Sciences, University of the Western Cape, Private Bag X17, Bellville 7535, South Africa; tidube@uwc.ac.za
* Correspondence: kiletashoko@gmail.com; Tel.: +27-78846-4673

Received: 7 February 2018; Accepted: 26 February 2018; Published: 6 April 2018

Abstract: While satellite data has proved to be a powerful tool in estimating C3 and C4 grass species Aboveground Biomass (AGB), finding an appropriate sensor that can accurately characterize the inherent variations remains a challenge. This limitation has hampered the remote sensing community from continuously and precisely monitoring their productivity. This study assessed the potential of a Sentinel 2 MultiSpectral Instrument, Landsat 8 Operational Land Imager, and WorldView-2 sensors, with improved earth imaging characteristics, in estimating C3 and C4 grasses AGB in the Cathedral Peak, South Africa. Overall, all sensors have shown considerable potential in estimating species AGB; with the use of different combinations of the derived spectral bands and vegetation indices producing better accuracies. However, WorldView-2 derived variables yielded better predictive accuracies (R^2 ranging between 0.71 and 0.83; RMSEs between 6.92% and 9.84%), followed by Sentinel 2, with R^2 between 0.60 and 0.79; and an RMSE 7.66% and 14.66%. Comparatively, Landsat 8 yielded weaker estimates, with R^2 ranging between 0.52 and 0.71 and high RMSEs ranging between 9.07% and 19.88%. In addition, spectral bands located within the red edge (e.g., centered at 0.705 and 0.745 µm for Sentinel 2), SWIR, and NIR, as well as the derived indices, were found to be very important in predicting C3 and C4 AGB from the three sensors. The competence of these bands, especially of the free-available Landsat 8 and Sentinel 2 dataset, was also confirmed from the fusion of the datasets. Most importantly, the three sensors managed to capture and show the spatial variations in AGB for the target C3 and C4 grassland area. This work therefore provides a new horizon and a fundamental step towards C3 and C4 grass productivity monitoring for carbon accounting, forage mapping, and modelling the influence of environmental changes on their productivity.

Keywords: WorldView-2; Landsat 8; Sentinel 2; *Festuca costata*; *Themeda triandra*; productivity

1. Introduction

C3 and C4 grass species Aboveground Biomass (AGB) indicates the productivity of grasses with common phenological, physiological, and morphological characteristics [1,2]. The accumulation and availability of C3 and C4 grasses AGB offers a wide range of ecosystem goods and services, as well as influence varying environmental processes. For instance, they are forage sources for a vast array of wildlife and livestock populations [3], provide a fuel load [4], maintain biodiversity, and are potential carbon pools [5]. C3 and C4 grass species are, however, facing considerable threats from environmental changes and these are anticipated to vary significantly, according to species functional types [6,7]. Most importantly, as they have different environmental tolerances and requirements, C3 and C4 AGB will respond differently to environmental changes, anthropogenic pressure, management

practices, and invasion. Similarly, considerable uncertainties about the productivity of C3 and C4 grass species also exist under a carbon dioxide-enriched, warmer environment and the influence of local conditions [8]. Consequently, there is a need to identify robust methods, which have the ability to spatially and temporarily characterize the AGB of these grasses, with better and reliable accuracies. This is critical to improve the monitoring of C3 and C4 grasses' productivity, and the associated response to environmental and anthropogenic pressure.

Field measurements and experimental surveys have, so far, been the prominent approaches used to determine C3 and C4 grasses' AGB for various applications [4,9,10]. However, these approaches are labour-intensive and very expensive, which has limited their full operationalization, especially in the developing world. In addition, they lack spatial representation [11–13], which is insufficient for spatial and temporal monitoring. The use of remotely sensed data remains the feasible method to estimate and spatially characterize C3 and C4 grass species AGB, for large areas, in a cost effective manner [12,14]. The review by Shoko et al. [15] has provided a much needed overview on the progress of the remote sensing of C3 and C4 grass species AGB. The review identified detailed findings on the availability of sensors, their potential and limitations, and the challenges and prospects for C3 and C4 grass species AGB monitoring. In summary, it was found that finding a cost-effective sensor, with a sufficient spatial resolution, and more and unique spectral bands, at a large geographical coverage for estimating C3 and C4 grass species AGB, is a major challenge that has discouraged the remote sensing community to continuously monitor these ecosystems. For example, previously-used sensors, such as the Advanced Very High Resolution Radiometer (AVHRR), have a very limited number of bands, which limits their spectral potential in differentiating C3 and C4 species characteristics. Their coarse spatial resolution, such as that of the Moderate-resolution Imaging Spectro-radiometer (MODIS at 1 km), misrepresents spatial variations in AGB.

It was also identified that new generation sensors, such as Landsat 8, RapidEye, WorldView-2, and Sentinel 2, with improved and unique characteristics, provide an invaluable opportunity to detect and quantify variations in AGB across grassland compositions of different photosynthetic types [15]. These sensors present more advanced remotely-sensed data to the remote sensing community, which has been caught in between the image acquisition cost, spatial coverage (which include spatial resolution and swath width), spectral capabilities, and accuracy, in predicting species AGB. More spectral bands constituted by these sensors (e.g., 13 from Sentinel 2) provide wide spectral windows to capture C3 and C4 AGB variations. Similarly, more spectral bands with different capabilities increase the sensitivity of the sensor to species phenological, physiological, and morphological characteristics, which influence AGB. The unique red edge bands have been acknowledged in species AGB estimation, due to their sensitivity and ability in providing additional relevant species information [16,17]. This is very important, especially considering the different physiological, morphological, and phenological properties of C3 and C4 grasses and the associated influence in AGB variations. For example, the phenological contrast between C3 and C4 has been documented. C3 grasses are typically present in the cool season, most active under cool conditions, and remain active throughout the year. C4 are warm season grasses mostly active during summer conditions and become dormant during winter. Similarly, the review by Adjorlolo [6] has highlighted the morphological differences in leaf anatomy between C3 and C4 grasses, which influences their ability to scatter, reflect, or transmit incoming radiation. Slaton et al. [18] also noted that typically, C4 grass leaves are significantly thinner, with long palisade cells, which reflect more radiation in the near infrared portion, compared to C3. On the other hand, C3 grasses have thick walls, which are normally associated with short, cylindrical mesophyll cells. The review by Shoko et al. [15] also reviewed the influence of these contrasts in estimating C3 and C4 grass species AGB. These contrasts in leaf anatomy require remote sensing variables which have the ability to differentiate for optimal AGB estimation. So far, the readily-available Sentinel 2 provides easy access to high resolution red edge bands, which are currently available in commercial satellites [19,20]. These bands have the ability to extract subtle differences between species, so their inclusion will enhance the accuracy of AGB estimation.

The spatial properties of available sensors (e.g., 1 km^2 pixel resolution of AVHRR and MODIS), which have been the primary data sources for estimating C3 and C4 AGB, have also been limiting the accurate quantification and mapping of these grasses' AGB. The spatial resolutions of the Sentinel 2 (10 m) and Landsat 8 (30 m) are far better for characterizing C3 and C4 grass species AGB. These pixel resolutions enable better spatial representation of species AGB, which might be under- or over-estimated at a 1 km pixel resolution. Also, considering the co-existence of C3 and C4 grass species, sensor spatial resolution becomes a critical concern to capture AGB variations from these grasslands. In addition, a large swath width (e.g., 185 km for Landsat 8 and 290 km for Sentinel 2) allows monitoring at a large geographical coverage, whereas the associated high spatial resolution for Sentinel 2 is indispensable; hence these sensors hold much appeal for C3 and C4 grass species AGB estimation. This study therefore assessed the performance of new generation sensors, with refined earth imaging properties in estimating and mapping C3 and C4 grasses' AGB variations in the temperate region of KwaZulu-Natal, South Africa.

2. Methodological Approach

2.1. Study Site

AGB estimation for C3 and C4 grass species was conducted within the Drakensberg area of KwaZulu-Natal, which is one of the key natural grassland ecosystems in South Africa [4]. The area is predominantly grassland, with patches of Afromontane forests and rocky out crops. The study area (Figure 1) experiences wet and humid summers, extending from November to March [21], with varying rainfall ranging between 990 and 1130 mm [22]. The area also experiences dry and cold winters, from May to August, and is also characterized by regular frosts and snowfall [23]. Temperatures also vary, with a minimum of 5 °C in winter and a maximum of 16 °C in summer [4]. The topography of the area is highly diverse, with elevation between 1225 and 3034 m; as derived from the Advanced Spaceborne Thermal Emission and Reflection Radiometer (ASTER) digital elevation model (DEM). These characteristics influence AGB variations across the area.

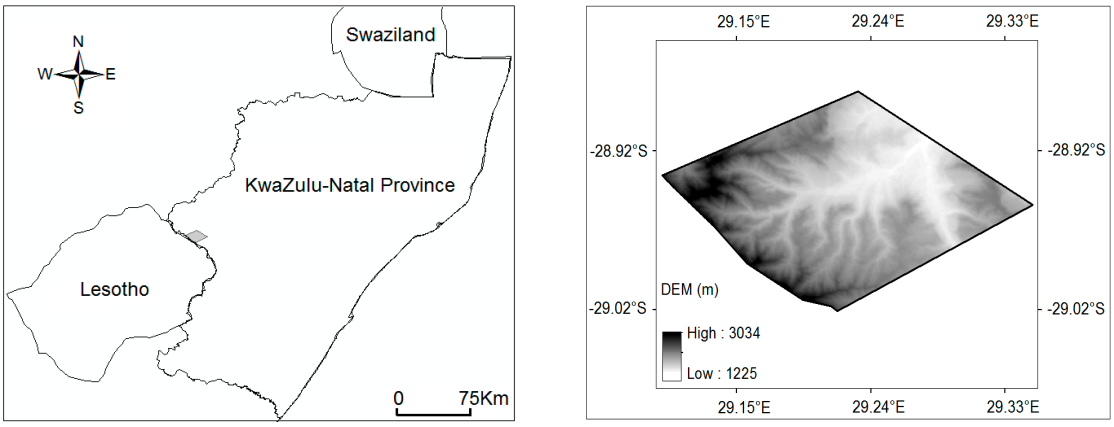

Figure 1. Location of the study area (**a**) and its altitudinal variations (**b**) [20].

2.2. Grass Species AGB Data Collection

The target grass species; *Festuca costata*, C3, and *Themeda triandra*, C4, are illustrated in Figure 2. These will be referred to as *F. costata* and *T. triandra* thereafter. The collection of AGB for these species was conducted from 10 to 17 February 2016, using 80 randomly generated points for each species. At each point, three quadrats measuring 50 cm × 50 cm were randomly thrown within a 10 by 10 m plot. This quadrat has been regarded as providing representative samples for AGB prediction, especially in predominantly grassland areas [24–26]. In each quadrat, standing grass was harvested and its weight

was determined in situ. The grass AGB samples were then transported and oven dried in grassland facilities, at the University of KwaZulu-Natal, to determine dry AGB which was then converted to kilograms per square meter (kg/m^2). A total of 240 AGB samples for each species was used for analysis. AGB sample x and y locations were also captured and recorded, at a sub-meter accuracy, using a Trimble GEO XH 6000 handheld global position system (GPS) (manufactured by Trimble Navigation Limited, Westminster, CA, USA).

(**a**) (**b**)

Figure 2. *F. costata* (**a**) and *T. triandra* (**b**) dominated landscapes (February 2016).

2.3. Remote Sensing Data Characteristics and Processing for AGB Estimation

Three images were acquired, with one each for the Landsat 8, Sentinel 2, and WorldView-2 multispectral sensors. Detailed information on the remote sensing image acquisition dates and the corresponding field data collection of species AGB is tabulated in Table 1. Landsat 8 images are delivered as raw digital numbers in the Universal Transverse Mercator (UTM) system. The sensor acquires 12-bit images at a 16-day revisit time, using the visible range, NIR, SWIR, and TIR, at a spatial resolution of 30 m. The calibration of Landsat 8 images was performed as highlighted on the website (http://landsat.usgs.gov/). The image was also corrected for atmospheric effects to derive surface reflectance, using the Fast Line-of-sight Atmospheric Analysis of Spectral Hypercube (FLAASH) model in the ENVI environment. Seven bands from the Landsat 8 were used in AGB estimations and these correspond to coastal blue (0.435–0.451 µm), blue (0.452–0.512 µm), green (0.533–0.590 µm), red (0.636–0.673 µm), NIR (0.851–0.879 µm), and the two SWIR (1.566–1.6512, 107–2294 µm), which have been considered by previous studies, not only in monitoring C3 and C4 grasslands [20,24], but in grassland areas [27,28].

Sentinel 2 is an open and freely-accessible multispectral data source, acquiring 12-bit images, every 5–19 days, at a 10 m, 20 m, and 60 m spatial resolution, in 13 spectral bands. Four bands delivered at a 10 m spatial resolution are centered at 0.49, 0.56, 0.665, and 0.842 µm. The 20 m spatial resolution six bands are centered at 0.705, 0.74, 0.783, 0.865, 1.375, and 2.190 µm, whereas three bands at a 60 m resolution are centered at 0.443, 0.945, and 1.375 µm. The Sentinel 2 image was provided in orthorectified top of atmosphere reflectance, with the UTM system, associated with the World Geodetic ellipsoid 84. The atmospheric correction of the image was also performed using the Sen2Cor atmospheric correction toolbox, which is an inbuilt algorithm within the Sentinel Application Platform (SNAP) tool. The tool was developed primarily to work with Sentinel images. The three bands acquired at a 60 m spatial resolution were excluded from the analysis, as they are primarily designated for atmospheric monitoring purposes [29], whereas the 20 m spatial resolution bands were resampled to 10 m of the rest of the bands. The resampling was performed in SNAP using the nearest neighbor resampling tool. A WorldView-2 commercial image was purchased and it was delivered after all the necessary corrections were performed by the supplier. The image was acquired at a 2 m spatial resolution in eight spectral ranges corresponding to coastal blue (0.4–0.45 µm), blue (0.45–0.51 µm),

green (0.51–0.581 µm), yellow (0.585–0.625 µm), red (0.63–0.69 µm), red edge (0.705–0.745 µm), NIR (0.77–0.895 µm), and NIR 2 (0.86–1.04 µm) [30].

It remains a challenge to obtain three different remote sensing datasets, with the same acquisition date, due to their varying revisit time. For example, within a month, only two images are available from the Landsat 8, with a 16-day revisit time. However, for Sentinel 2, there are high possibilities of obtaining more images within a month, with its high revisit frequency of five days. In addition, the influence of cloud cover also hinders the acquisition of corresponding images, especially during the summer period. However, although the images had different acquisition dates, they were all collected within the same week and seasonal period during the summer. Only one image for each dataset was acquired and used in this study. Although more images are required for better vegetation classification, the intention of the study was to compare the performance of newly-launched Sentinel 2 and Landsat 8. In addition, different studies elsewhere have yielded reasonable results in assessing the performance of different sensors, using a single image dataset, acquired within the same season. Secondly, it remains a challenge to acquire more images for WorldView-2 commercial data, due to its acquisition cost.

Table 1. Summary of datasets acquired and used in this study.

Field Data Collection Period	Remote Sensing Dataset	Acquisition Date	Supplier/Source
10–17 February 2016	Landsat 8	16 February 2016	USGS GloVis https://glovis.usgs.gov/
	Sentinel 2	12 February 2016	Sentinels Scientific Data Hub archive https://scihub.copernicus.eu/
	WorldView-2	16 February 2016	Purchased from Digital Globe, Longmont, CO, USA

To derive AGB maps for the target species, without other land cover or grass classes, image classification was performed. The classification was done using the species GPS points collected as training samples, whereas other land cover classes within the study area were masked out to show AGB variations for the target grass species only. In a separate study [19], the potential of Landsat 8, Sentinel 2, and WorldView-2 in discriminating the target species was investigated, using images acquired in summer, which were used to estimate the AGB in this study. The detailed information for the classification procedure, associated variables, and accuracy results are provided by Shoko and Mutanga [19]. The final output map for the two grass species was derived using the standard NDVI, which showed a great performance when compared to other indices that were considered in the study.

2.4. Regression Algorithm for Predicting F. costata and T. triandra Grass Species AGB

This study used the Sparse Partial Least Square Regression (SPLSR) [31] to predict AGB variations using Landsat 8, Sentinel 2, and WorldView-2 multispectral datasets. SPLSR is a robust and powerful algorithm for estimating vegetation biophysical properties using remote sensing data. So far, its high performance in predicting grass AGB across different environments has been reported [32–34]. The model builds estimation functions and associated variables using remote sensing datasets. The model achieves this through transformation of the remote sensing variables to a set of components and variables, which show their ability in estimating AGB [27]. To determine the number of components for optimal results in estimating species AGB, the leave-one-out cross-validation (LOOCV) approach was used. The cross validation was done using 30% of the AGB data collected from the field. The optimum number of components searched for each variable set was between 1 and 10, as recommended by Chun and Keleş [31]. The approach produced estimation errors, using the Root Mean Square Error of Prediction (RMSEP) associated with a certain number of components. The component and associated variables with the lowest estimation errors were then considered for further analysis

and the AGB estimation. The same approach was used successfully, for example, by Sibanda et al. [27], Abdel-Rahman et al. [34], and Kiala et al. [35].

The SPLSR was run using single species datasets separately and a combined species dataset. The single species dataset comprised individual species AGB for *F. costata* and *T. triandra* grasses, separately. Secondly, the model was run using pooled data, where the *F. costata* and *T. triandra* species dataset was combined. This was performed to produce integrated species AGB models for mapping. Before the model was run, the field-based AGB data samples were split into 70%, which was used to train the model, whereas the remaining 30% was used for validation. This is a requirement when estimating vegetation biophysical properties using machine learning algorithms. All the computations of the SPLSR model were run using R software. The model also provided the most optimal variables for estimating AGB, by means of variable scores, where variables with scores above 1 were regarded as the most important, while those below 1 were less important. The SPLSR output includes a model that is used for AGB calculation with remote sensing images within a Geographic Information System environment. In this study, the AGB maps were produced using ARCGIS 10.2. (ESRI; New York, NY, USA) software based on the model derived using SPLSR.

2.5. Remote Sensing Variables for Estimating Grass Species AGB

Three sets of variables derived from Landsat 8, Sentinel 2, and WorldView-2 sensors, as illustrated in Table 2, were used to predict AGB, using the SPLSR model. Vegetation indices that were used to predict AGB for the target grasses were chosen based on their performance in estimating AGB for C3 and C4 grass species compositions [2,36,37]. In addition, the red edge-based simple ratio and NDVI, which were previously reported [25] to perform well across grassland ecosystems in general, were adopted to predict AGB variations for C3 and C4 grass species. This provides more insight about the potential of the unique bands in deriving these indices differently, which have been primarily developed using the visible portion of broadband multispectral datasets.

In analyses i and ii, individual variables were used in isolation to predict species AGB. Thus for analysis I, which included the use of spectral bands only from the three sensors, the model was run with field-based species AGB values and their corresponding reflectance values. For analysis ii, only indices were used to estimate species AGB, whereas in analysis iii, all the bands and indices were combined with their corresponding field-based species AGB.

In addition, sensors data fusion was done, where all the variables from each sensor were combined and used in the model. This was performed using the three variables which included all sensors (i) bands, (ii) indices, and (iii) bands plus indices. This provides a more comprehensive insight of the competence of each sensor's variables in estimating C3 and C4 grass species AGB, than when the sensor variables are used in isolation. Additionally, data fusion provides the most important bands or indices across multispectral sensors.

Table 2. Remote sensing variables used to predict species AGB for C3 and C4 grass species compositions.

Data Type	Details	Analysis Set
Landsat 8 Sentinel 2 WorldView-2	Seven spectral bands (CB, B, G, R, NIR, SWIR1, SWIR2) Ten spectral bands (B, G, R, RE1–3, NIR, RE4, SWIR1, SWIR2) Eight spectral bands (CB, B, G, Y, R, RE, NIR1, NIR 2)	i
Vegetation Indices (VIs)	EVI, SAVI, StNDVI, RDVI, SR, MSR (common to all sensors) NDVIRE1–4, SRRE1–4 (using Sentinel 2 red edge bands) NDVIRE, SRRE (using WorldView-2 NIR1 and RE) NDVI2 and SR2, (using WorldView-2 NIR2 and R) NDVIRE2, SRRE2 (using WorldView-2 NIR2 and RE)	ii
Image spectral data + VIs	Combined image spectral bands and vegetation indices	iii

EVI: Enhanced vegetation index [38], SAVI: Soil adjusted vegetation index [39], StNDVI: standard NDVI [40], RDVI: renormalized difference vegetation index [41], SR: simple ratio [42].

Table 3 illustrates the formulas for all the indices used for estimating species AGB using Landsat 8, Sentinel 2, and WorldView 2 datasets. The indices were differentiated with the prefixes L8, S2, and WV2, indicating Landsat 8, Sentinel 2, and WorldView-2 data sources.

Table 3. Indices used derived from the three sensors' spectral bands.

Vegetation Index	Formula	Details
EVI	2.5 ((NIR − R)/(1 + NIR + 6R − 7.5 × B))	Common to all sensors
SAVI	((NIR − R) × (1 + L))/(NIR + R + L)	
Stnd NDVI	(NIR − R)/(NIR + R)	
RDVI	(NIR − R)/Sqrt (NIR + R)	
Simple ratio	NIR/R	
MSR	(NIR/R − 1)/Sqrt (NIR/R) + 1	
NDVIRE1	(NIR − RE1)/(NIR + RE1)	Sentinel 2 red edge-derived NDVI and SR
NDVIRE2	(NIR − RE2)/(NIR + RE2)	
NDVIRE3	(NIR − RE3)/(NIR + RE3)	
NDVIRE4	(NIR − RE4)/(NIR + RE4)	
SRRE1	NIR/RE1	
SRRE2	NIR/RE2	
SRRE3	NIR/RE3	
SRRE4	NIR/RE4	
NDVIRE1	(NIR − RE)/(NIR + RE)	WorldView-2 red edge and additional NIR-derived NDVI and SR
SRRE1	NIR/RE	
NDVI2	(NIR2 − R)/(NIR2 + R)	
SR2	NIR2/R	
SRRE2	NIR2/RE	

Sqrt: squareroot, L: constant.

2.6. Species AGB Estimation Accuracy Assessment

Statistical measures of AGB estimation accuracy using the different sensors and associated variables were determined, as well as the model performance in estimating species AGB. These measures included the coefficient of determination (R^2), root mean square error (RMSE), and RMSE%. The RMSE is a measure of the difference between the actual measured AGB values in the field and the estimated values. These are frequently used in prediction accuracy assessments using remote sensing data. The *RMSE* was calculated using the formula:

$$RMSE = \sqrt{\frac{\sum_{i-1}^{n}\left(X_{measured} - X_{predicted}\right)^2}{n}} \quad (1)$$

where: $X_{measured}$ is the measured AGB, $X_{predicted}$ is the predicted AGB, and i is the predictor variable included. The *RMSE%* was also calculated as:

$$RMSE\% = \frac{\sqrt{\frac{1}{n}\sum_{1=n}^{n}(y_i - \hat{y}_i)^2}}{\overline{y}} \times 100 \quad (2)$$

where n is the number of measured values, y_i is the measured value, $\hat{y}_i$ represents the estimated values, and $\overline{y}$ is the mean of the measured AGB. These formulas were adopted from Dube and Mutanga (2015).

A better model using the different metrics was selected from each sensor based on the highest R^2 and lowest RMSE. The selected model and associated variable with the highest VIP score for each sensor were then used to produce AGB maps for the study area in ARCGIS 10.2. Significant difference tests were also performed to determine if the performances of the three sensors in estimating C3 and C4 grass species AGB were significantly different. In addition, it was also tested whether the estimation accuracies of *F. costata* was significantly different from that of *T. triandra*, using the three sensors.

3. Results

3.1. Species AGB Variations Measured

Table 4 shows the descriptive statistics of measured *F. costata* and *T. triandra* grass species AGB. It was found that in early February, *T. triandra* grass had higher AGB variations, when compared to *F. costata*. The measured AGB of *T. triandra* varied from 0.6 kg/m^2 to as high as 1.276 kg/m^2, whereas for *F. costata*, it varied between 0.52 kg/m^2 and 1.16 kg/m^2.

Table 4. Descriptive statistics of the measured species AGB (kg/m^2).

Species	*N* *	Minimum	Maximum	Average	Stdev.
F. costata	80	0.524	1.160	0.709	0.115
T. triandra	80	0.600	1.276	0.884	0.125
Combined species	160	0.524	1.276	0.797	0.148

* *N* is the number of sampled plots.

3.2. The Performance of Landsat 8, Sentinel 2 and WorldView-2 Variables in Predicting Species AGB

The results in Table 5 provide the performance of the variables derived from the three sensors in estimating species AGB. Overall, all the variables showed considerable potential in predicting species AGB. However, the WorldView-2 sensor produced the best prediction accuracies, with the least estimation errors (between 6.92% and 9.84%), followed by Sentinel 2 estimates, which were far better than those obtained using the Landsat 8 sensor. Spectral bands from all the sensors also estimated species AGB with the lowest accuracies, when compared to the use of indices and combined variables. There were noticeable improvements in the estimation accuracy, from using spectral bands, to the use of combined variables, for both individual species and combined species datasets. This was most evident for Landsat 8 and Sentinel 2. For instance, Landsat 8 derived spectral bands produced an R^2 of 0.55 (RMSE = 17.55% of the mean) when estimating *F. costata* AGB. When estimating for *T. triandra*, an R^2 of 0.52 was produced, with an RMSE of 19.88%. Landsat 8 bands also estimated combined species with an R^2 of 0.52 and an RMSE of 18.19%. When using indices, R^2 improved to 0.68 for *F. costata*, 0.63 for *T. triandra*, and 0.65 for combined species, whereas the errors of estimation were reduced to 11.48%, 12.53%, and 13.5% for *F. costata*, *T. triandra*, and the combined species dataset, respectively.

Tests of significance according to the *t*-test also revealed that the three sensors had significant differences in estimation accuracies using the different variables. Significant differences ($\alpha < 0.05$) were only observed between sensors, as well as between the variables used. However, although slight differences between the two species were observed, the differences were not significant ($\alpha < 0.05$).

Figure 3 shows the predictive accuracies of species AGB using optimal variables from the three sensors. These graphs illustrate the relationships between measured and estimated AGB, using combined variables, which were found to have better estimation accuracies, when compared to the use of spectral bands or indices. The optimal variables include Landsat 8 NDVI, NIR, and SWIR; Sentinel 2 red edge bands (centered at 0.705, 0.74, and 0.783 μm) with derived indices, NIR, and SWIR, whereas for the WorldView-2, it was NIR, red and red edge bands, and derived indices.

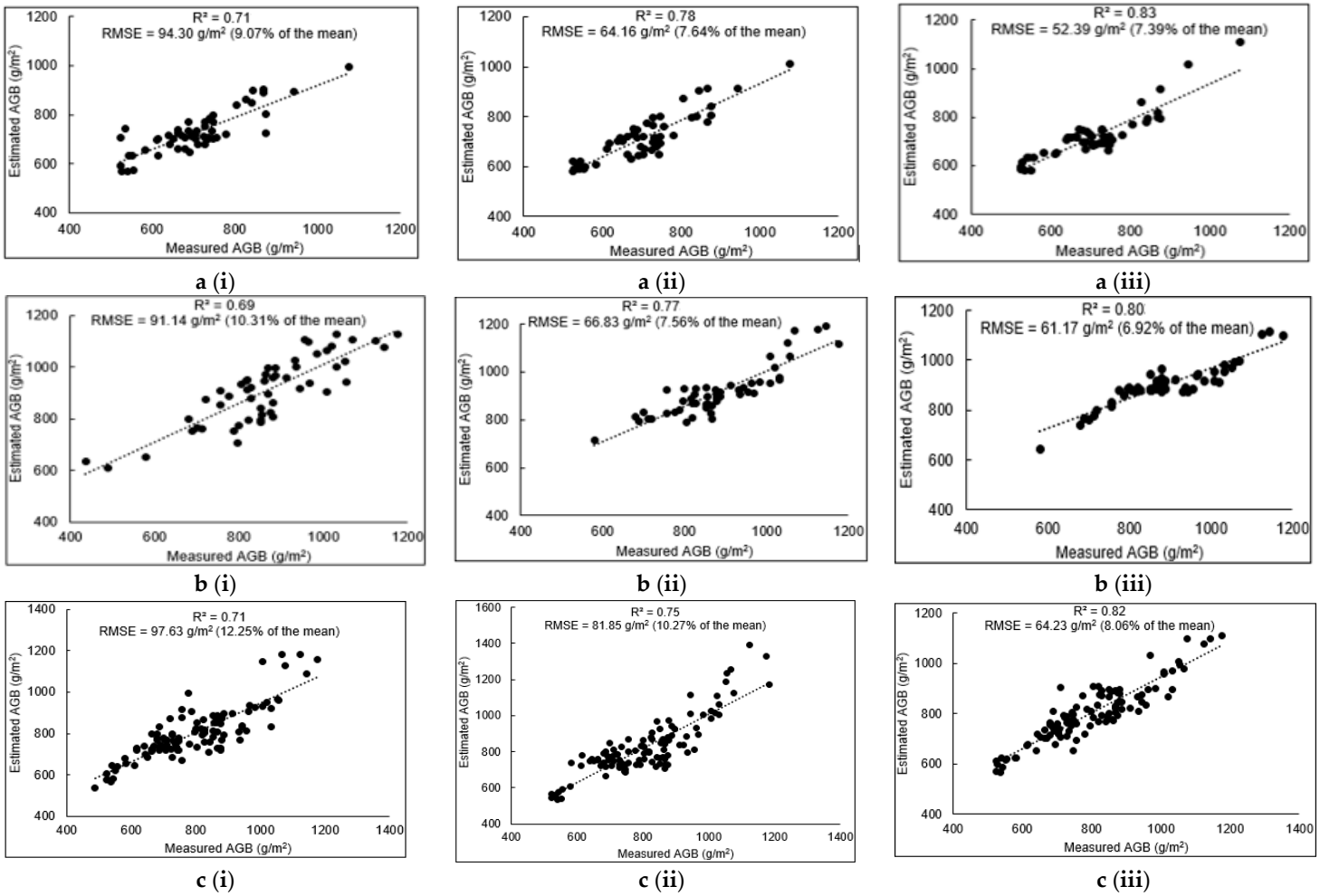

Figure 3. The relationship between species combined measured and estimated AGB using the optimal variables of the three remote sensing datasets. (**a**–**c**) represent *F. costata*, *T. triandra*, and combined species dataset, respectively. (**i**–**iii**) represent Landsat 8, Sentinel 2, and WorldView-2 datasets, respectively.

Table 5. Sensor AGB predictive accuracies for *F. costata*, *T. triandra*, and combined species.

Remote Sensing Datasets	*F. costata*			*T. triandra*			Combined Species		
	R^2	RMSE (g/m^2)	RMSE (%)	R^2	RMSE (g/m^2)	RMSE (%)	R^2	RMSE (g/m^2)	RMSE (%)
Bands									
Landsat 8	0.55	164.42	17.55	0.52	175.73	19.88	0.52	150.63	18.91
Sentinel 2	0.61	145.85	13.11	0.60	129.59	14.66	0.61	122.74	15.04
WorldView-2	0.73	93.59	8.97	0.71	97.50	9.22	0.72	78.42	9.84
Indices									
Landsat 8	0.68	101.39	13.48	0.63	110.76	12.53	0.65	107.59	13.51
Sentinel 2	0.76	91.19	10.49	0.74	93.62	9.46	0.71	84.8	10.64
WorldView-2	0.79	55.44	7.82	0.77	64.17	7.26	0.75	64.47	8.09
Combined Variables									
Landsat 8	0.71	94.3	9.07	0.69	91.14	10.31	0.71	97.63	12.25
Sentinel 2	0.79	64.16	7.64	0.77	66.83	7.56	0.74	81.85	10.27
WorldView-2	0.83	52.39	7.39	0.8	61.17	6.92	0.82	64.23	8.06

These results were based on the 70% sample set.

3.3. Model Validation Results

Figure 4 provides the performance of the model in estimating species AGB using the independent 30% validation set. Overall, the SPLSR performed well in estimating species AGB and the results were comparable to those produced using the 70% set. Therefore, only the validation results for optimal variables for species pooled data were shown.

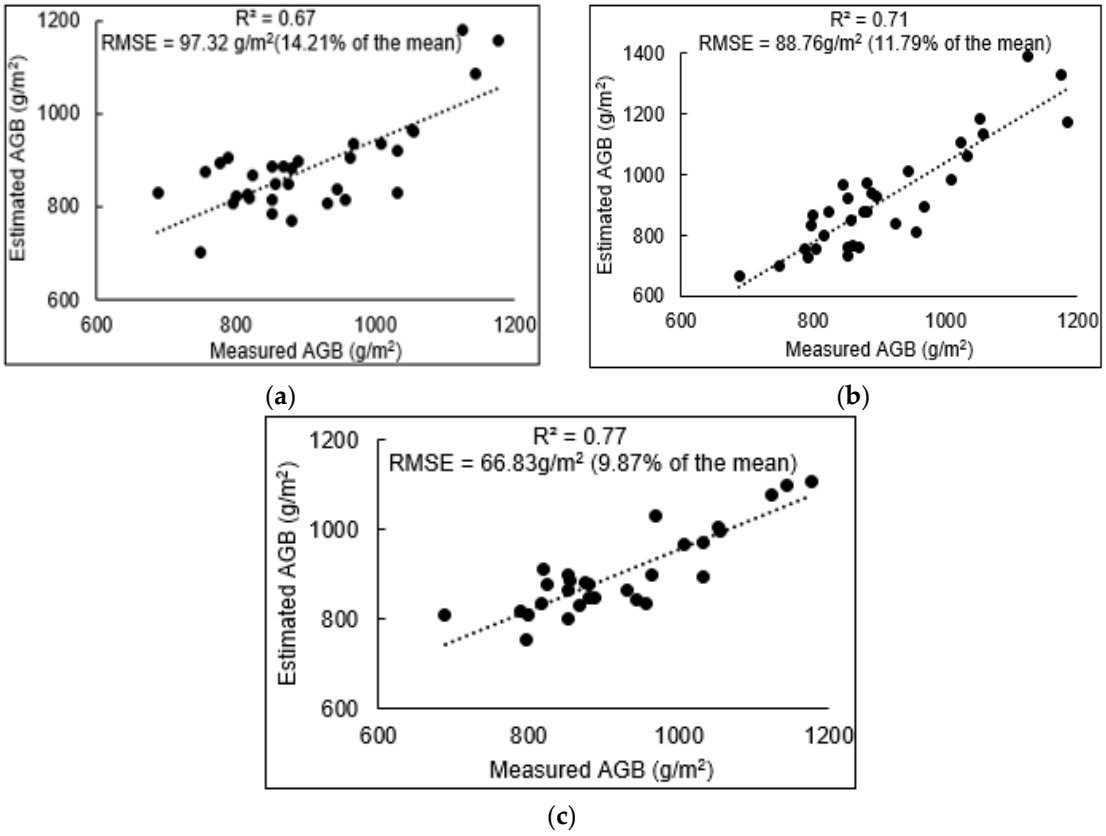

Figure 4. Model performance in estimating species AGB. (**a**–**c**) represents Landsat 8, Sentinel 2, and WorldView-2 remote sensing datasets.

3.4. Sensors Data Fusion Results in Predicting C3 and C4 Grass Species AGB

When all the bands and indices from the three sensors were used separately for the individual species dataset, the maximum number of components was two. Therefore, a report for the component with the lowest RMSEP and associated variables was provided. Figure 5 provides the most variables selected after fusing the three datasets, at an individual species level and using species pooled data. S2, L8, and WV2 represent Sentinel 2, Landsat 8, and WorldView-2 sensors, respectively. Overall, the results indicated that the NIR, red edge, and SWIR bands were the most important bands across sensors. When indices were used, the standard NDVI from Landsat 8 was found among the most important indices of Sentinel 2 and WorldView-2, which included red edge-based indices. At an individual species level, more variables were selected as important for estimating *F. costata* AGB, whereas for the *T. triandra* and pooled species dataset, a few variables were selected. However, when the variables selected from data fusion were applied in estimating C3 and C4 grass species AGB, the results in terms of R^2 and RMSE did not improve significantly; thus, they were not reported in this study.

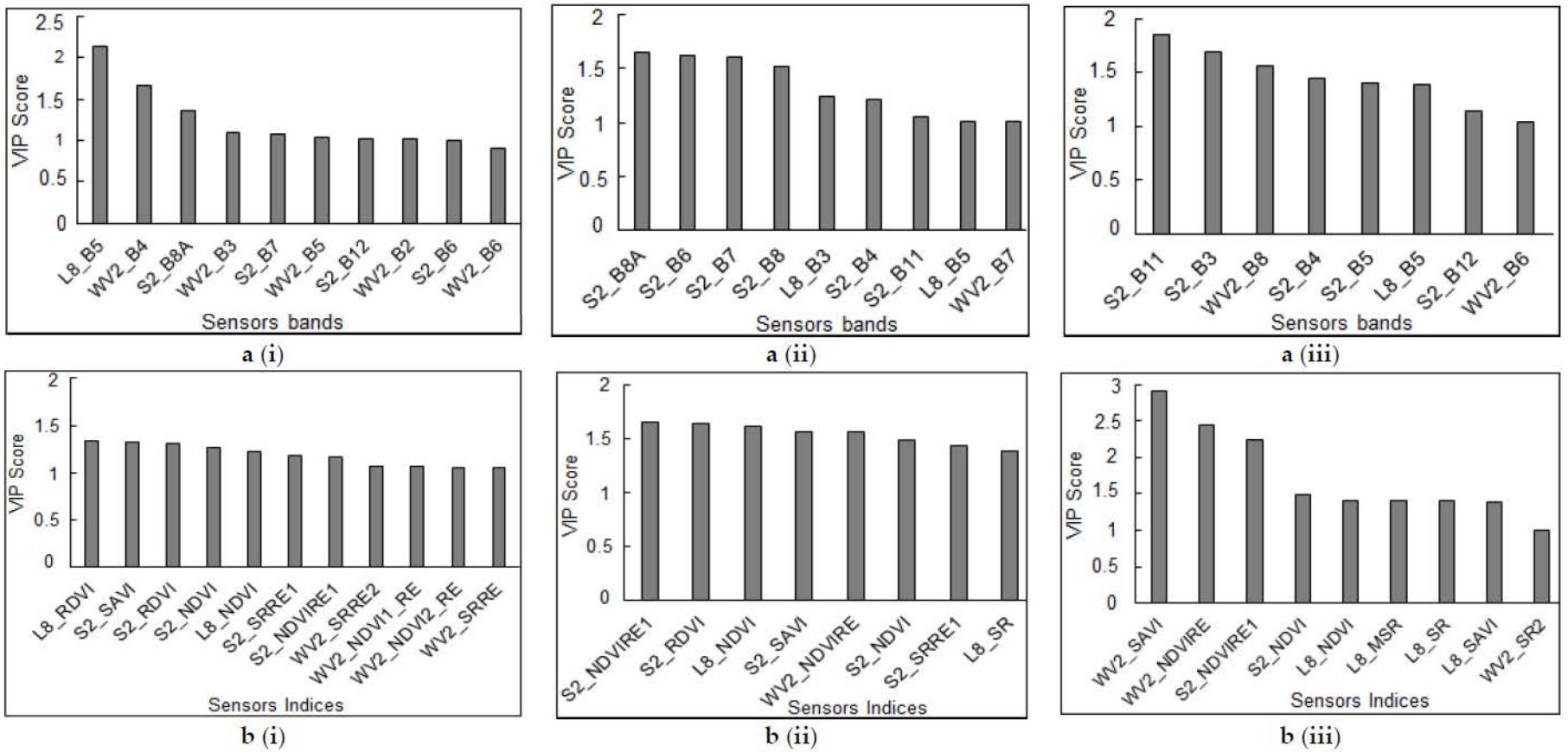

Figure 5. The most important (**a**) bands and (**b**) indices for estimating (**i**) *F. costata*, (**ii**) *T. triandra*, and (**iii**) combined species AGB across sensors.

3.5. The Potential of the Sensors in Predicting and Mapping C3 and C4 Grasses AGB

Figure 6 shows the spatial variations of species AGB, estimated using optimal variables of the three multispectral sensors and species combined dataset. The combined species dataset has shown that NDVI was the most influential in estimating AGB. However, the index was derived using different sensors' spectral bands. For the Landsat 8 (a), the AGB map was derived, using the standard NDVI, whereas for Sentinel 2 (b), NDVI derived using red edge centered at 0.705 µm was used and the NDVI using the red edge (centered between 0.705 and 0.745 µm) was also used for WorldView-2 (c). Thus, NDVI derived using different spectral bands from the three datasets was used for species AGB mapping across the study area.

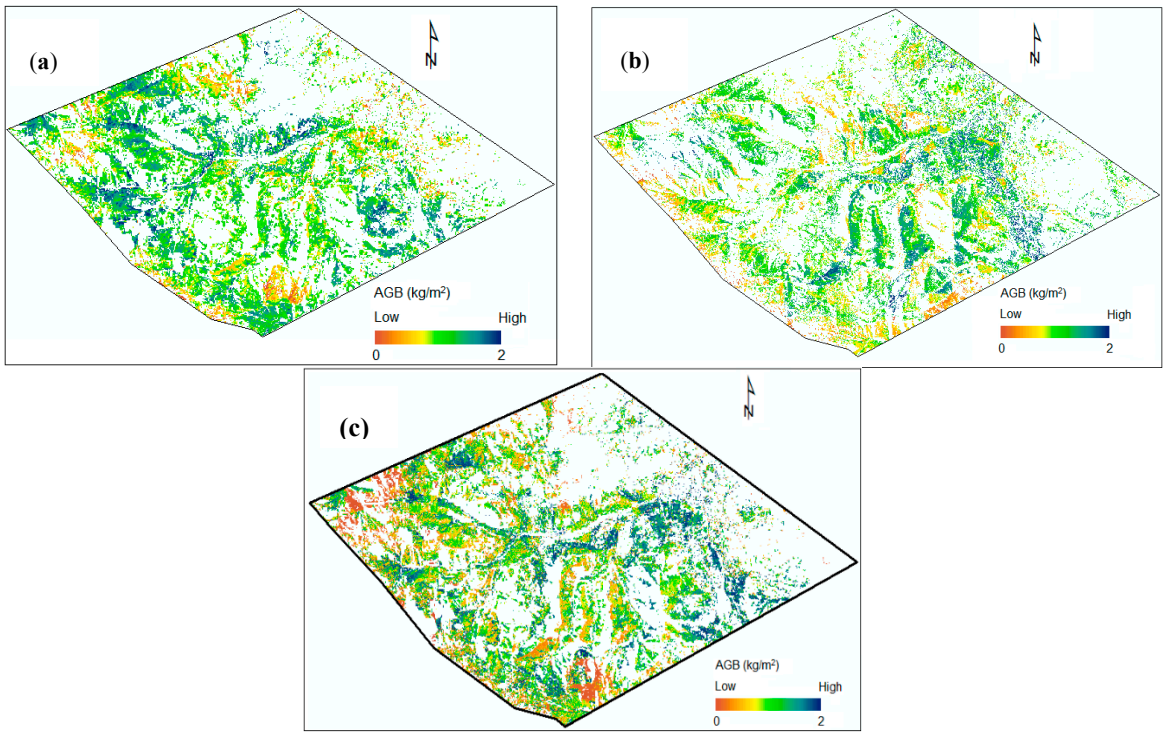

Figure 6. AGB variations in February 2016, derived using (**a**) Landsat 8, (**b**) Sentinel 2, and (**c**) WorldView-2 remote sensing datasets.

4. Discussion

Remote sensing of C3 and C4 grass AGB has remained a challenge, due to the lack of data sources which have the capabilities to spatially characterize such subtle variations. The different physiological, morphological, and phenological properties of C3 and C4 grasses influence AGB variations. Previous reviews, for example, [6,15], have noted the differences in leaf anatomy between C3 and C4 grasses, which influence their ability to scatter, reflect, or transmit incoming radiation. Although these variations have been documented, not all sensors have the ability to discern such variations and estimate species AGB with optimal accuracy. This has resulted in a lack of continuous monitoring of their productivity. It is therefore of much importance to identify remote sensing datasets to quantify and map the productivity of C3 and C4 dominated grasslands across vast scales. Current developments in remote sensing offer new perspectives for C3 and C4 AGB monitoring and modelling. It is also the focus of the remote sensing community to shift towards the use of freely-available new generation sensors, which have emerged with better capabilities for improved AGB estimation and monitoring. Similarly, the continuous monitoring of grassland areas is also a

cause for research, especially in the light of climate change and its effects on food security, the carbon cycle, and biodiversity.

4.1. The Performance of Landsat 8, Sentinel 2, and WorldView-2 Variables in Predicting Species AGB

It can be observed that all sensors constitute variables which have the potential to estimate C3 and C4 grass species AGB. The availability of more bands from Sentinel 2 provides more spectral windows which are influential, as well as enabling the computation of different indices which have the potential to predict C3 and C4 grasses AGB. This has been reported by the findings of Addabbo et al. [43], which highlighted that the novel spectral bands of Sentinel 2 allow the computation of new indices, which offer additional information for vegetation analysis. The lower number of bands of the Landsat 8 sensor limits the number of variables with the potential to estimate AGB. Among the most important variables for predicting C3 and C4 grasses AGB were spectral bands. For example, the Landsat 8 NIR and SWIR, as well as the red edge of Sentinel 2 and WorldView-2, contributed to species AGB estimation. Thus, spectral bands of the new generation sensors have the capability to contribute to the estimation of C3 and C4 grasses AGB.

In addition, the important variables across the three sensors were mostly located within the NIR, red edge, and SWIR portions, as well as the corresponding indices. This was shown when individual sensors were tested, as well as from the fusion of the three datasets. However, for Landsat 8, only the NIR and derived indices and SWIR bands were competitive enough among Sentinel 2 and WorldView-2 variables. The potential of spectral bands of previously-used sensors has not been reported, as researchers were biased towards the use of derived indices, due to the broad spectral channels, which were perceived to be insensitive to species biophysical properties. However, a few studies reported the influence of the NIR band in C3 and C4 grass species monitoring using previous Landsat data series, like the Thematic Mapper 5 (TM 5) [44]. The study has highlighted significant differences in the NIR reflectance between C3 and C4 grass species using TM 5. In a different study, Lu et al. [45] also reported the importance of NIR in estimating C3 and C4 grass species AGB using AISA Eagle hyperspectral imagery in Japan. The contribution of the SWIR portions in AGB predictions has been reported in grasslands ecosystems. The study by Chen et al. [46] reported the significance of SWIR bands in predicting AGB in the semi-arid rangelands of Idaho. This might also encourage future work to consider the use of SWIR-based indices, especially when using Landsat 8 and Sentinel 2 sensors.

Similarly, red edge bands and derived indices have been found to be sensitive to the biophysical properties of species, hence they boost the prediction of species AGB, when compared with the visible channels [17,27,32]. The contribution of NIR, SWIR, and red edge in this study might be attributed to the varying concentration of leaf pigments (e.g., chlorophyll and water) between C3 and C4. For example, NIR and red edge are closely related to chlorophyll [47,48], whereas SWIR is closely related to water content [49]. These bands have also been reported to be closely related to species AGB variations [33], hence their important contribution in AGB estimation was observed in this study. This possibly indicates the variability in chlorophyll or water content between C3 and C4 species during the summer period, as indicated by a different study.

Spectral bands have a low AGB predictive accuracy, when compared to the use of derived indices and a combination of variables. Improved prediction accuracies using indices have been acknowledged in estimating species AGB by previous studies [32,45,50]. These variables have been perceived to be more sensitive to species characteristics, which improve their predictive accuracy, than individual bands. However, it should be noted that the performance of Landsat 8 spectral bands was weak, when compared to that of Sentinel 2 and WorldView-2. The slightly weaker performance of Landsat 8 bands in this study indicates the weaker performance of traditional bands in C3 and C4 dominated grasslands. In addition, Landsat 8 spectral setting lacks unique bands like red edge, which weakens its potential to predict species AGB. On the other hand, the Sentinel 2 and WorldView-2 sensors constitute unique and important bands, which have the ability to extract the varying bio-physical characteristics

of C3 and C4 species, which influence AGB. It should also be highlighted that the performance of traditional indices based on the traditional bands, such as visible or NIR, were less important, when compared to those indices that were derived using additional unique bands, such as red edge and NIR. Substantial studies [43,51] have studied the competence of indices derived from red edge or additional NIR, with those derived from traditional bands in characterizing the biophysical properties of species. For example, the study by Addabbo et al. [43], which compared Landsat 8-based NDVI (using the red and NIR) with Sentinel 2 red edge NDVI for characterizing different vegetation.

Most interestingly, the improved performance using vegetation indices and combined variables was most apparent for Landsat 8, when compared to Sentinel 2 or WorldView-2. This may be explained by the fact that Landsat 8 constitutes broad traditional bands, which are not detailed enough to predict AGB, so the inclusion of more than individual bands increases its prediction accuracy. In confirmation, vegetation indices have been the primary variables which have been preferred, over the use of individual bands, to estimate AGB variations between C3 and C4 grasses using broadband multispectral sensors [44,52–54]. Broadband indices have been identified to be more sensitive to species AGB, which cannot be sensed by individual bands, thereby improving the model predictive accuracy. So far, the application of Landsat data series in estimating C3 and C4 grasses AGB has been very limited, except for a few studies which reported the derived indices. For example, the study by Davidson and Csillag [55] in Canada reported the potential of the standard NDVI (R^2 = 0.64) from a Landsat TM 5-based Exotech Model radiometer, when compared to other indices. In a different study, in the Kansas state of the United States of America, Peterson et al. [44] reported that although NDVI was influential in estimating C3 and C4 grass species AGB, the index failed to significantly differentiate variations in AGB between the two grass species. In this regard, mixed findings have been reported from previously-used Landsat datasets.

Although the use of sensor fusion did not improve the estimation accuracies, it sheds more light on the competence of variables derived from the freely-available sensors in C3 and C4 AGB estimation. A previous sensors fusion approach has been widely applied in estimating forestry structural attributes and these studies used multispectral and LiDAR data. These studies have reported an improvement in forest AGB estimations [56,57]. The improved results were mainly attributed to the ability of LiDAR in providing vegetation vertical profiles (e.g., height), rather than multispectral datasets. In this regard, future work might consider the fusion of multispectral datasets used in this study with LiDAR.

4.2. The Potential of Landsat 8, Sentinel 2, and WorldView-2 to Predict and Map C3 and C4 Dominated Grasslands AGB

One of the challenges faced by researchers in monitoring C3 and C4 AGB has been the ability of available sensors to map subtle AGB variations. This has been shown by the scarcity of the distributional maps of C3 and C4 AGB variations. Previously-used sensors were inadequate; they provided unsatisfactory predictions, because of their coarse spatial resolution and broad spectral channels. For example, the studies by Tieszen et al. [2] and An et al. [14] using AVHRR NDVI predicted C3 and C4 AGB with coefficients of determination of 0.58 and 0.54, respectively, whereas Rigge et al. [36] reported AGB overlaps, using MODIS NDVI in the Prairies of the United States of America. Findings from this study have therefore shown improved estimations using the recently emerged multispectral sensors compared to those that have been previously reported.

To the best of our knowledge, AGB maps for C3 and C4 grass species are rarely available. So far, few studies have attempted to map C3 and C4 grasslands AGB using hyperspectral [45] and climatic variables [58]. However, the use of hyperspectral images, which are associated with a high acquisition cost and climatic data proved unsuccessful and did not receive enough attention in order to understand the spatial variations of C3 and C4 AGB over large areas, especially in Africa, where climatic observation networks are very poor and financial resources are limited. This has limited the availability of AGB maps for C3 and C4 grasses. This study has therefore revealed a new opportunity for estimating and mapping AGB in C3 and C4 dominated grasslands over large areas in a cost effective

manner, especially for the developing world, where the acquisition of commercial satellites is difficult. All three sensors showed great potential in mapping the spatial variations of species AGB. Researchers now have opportunities to use freely-available Sentinel 2 and Landsat 8 or a combination of these datasets in monitoring the productivity of C3 and C4 grass species for a variety of applications.

Findings from this study also reveal the anticipated performance and potential of new generation sensors in mapping the AGB variations of C3 and C4 grassland areas [15]. The sensors thus contain important abilities to monitor these grassland ecosystems, which was becoming almost impossible. Although it was not as good as the WorldView-2, Sentinel 2 was better than Landsat 8. For example, Sentinel 2 predicted species AGB with a better accuracy and showed better spatial variations compared to Landsat 8. Recently, the study by Addabbo et al. [43] reported the improved efficiency of the S-2, over that of Landsat 8. The study found statistically significance differences between the performances of the two sensors, using derived NDVI. They also reported that within a particular area, Sentinel 2 sampled 3015 pixels, when compared to 345 pixels from the Landsat 8. This confirms the magnitude of the Sentinel 2 10 m spatial resolution, in representing spatial variability.

The WorldView-2 was also confirmed to remain critical in predicting more accurately and mapping C3 and C4 species AGB, than Sentinel 2 and Landsat 8. Within the same area, the potential application of WorldView-2 in estimating and mapping C3 and C4 grass species canopy nitrogen, with satisfactory accuracy, has also been shown [30]. The high spatial resolution and associated unique spectral bands thus enable the sensor to capture the spatial variability in canopy characteristics, such as the leaf area index and pigment concentrations, which are related to species AGB variations; this improved its prediction accuracy. However, the operational application of the WorldView-2 might be hindered by its acquisition cost, which places Sentinel 2 and Landsat 8 as promising datasets for the monitoring of C3 and C4 grasses AGB, especially in data scarce environments.

Although reasonable predictive results were produced from this study, especially in relation to those accuracies reported using broad-band multispectral datasets, the performance of the model in predicting C3 and C4 species AGB cannot be ignored. Overall, the SPLSR produced good predictive results for all the sensors, using different variables. However, the results from this study might be considered inconclusive, since these sensors have been tested at a specific period. Snapshot AGB maps for C3 and C4 dominated grasslands are inadequate. This is because the AGB for these grasses varies over time, due to the influence of species phenology, and more importantly, changing climatic conditions. Decision making and the implementation of policies require more details of species AGB variations. In relation to the performance of the sensors, the ability of the sensor to predict and spatially represent species AGB might also be influenced by the period considered. There is therefore the need to show how these sensors (particularly the freely-available Sentinel 2 and Landsat 8 datasets) and the SPLSR model perform in predicting C3 and C4 grasses AGB, as well as their consistency over time.

5. Conclusions

The present study has shown the feasibility of using the new generation sensors to estimate and determine the subtle spatial variations of C3 and C4 grasses AGB in the temperate regions of South Africa. The most important finding from this study was the performance of the freely-available Landsat 8 and Sentinel 2 sensors in predicting grass species AGB. The sensors predicted species AGB with a high accuracy, which might be very useful in monitoring the productivity of C3 and C4 grasslands, for various applications and their conservation. The sensors provide significant data sources to enable the monitoring of C3 and C4 grass species productivity, across different ecosystems, especially for the developing world, where the acquisition of commercial datasets is a major limitation. These results are therefore encouraging for future efforts to continuously monitor and map C3 and C4 grasses' productivity at a large geographical coverage, over time.

Acknowledgments: Authors of this research are grateful to the European Space Agency and the National Aeronautics and Space Administration for the continual acquisition and freely-available Landsat 8 and Sentinel 2 satellite images. The assistance provided by Brice Gijsbertsen (UKZN) in acquiring WorldView-2 is greatly

appreciated. It is also a great pleasure to acknowledge the financial support provided by the Applied Center for Climate and Earth Systems Science and the National Research Foundation in South Africa. Authors also extend their gratitude to the SASSCAL Biodiversity task 131 for all the support provided. The Ezemvelo KwaZulu-Natal Wildlife is thanked for the provision of the research permit to access the area under study. The contribution of anonymous reviewers is highly appreciated; this has improved the paper.

Author Contributions: Cletah Shoko collected the data, performed the required analyses, and wrote the manuscript. The paper was compiled under the guidance and supervision of Onisimo Mutanga. Timothy Dube also helped with the analyses and manuscript editing, and provided necessary comments.

Conflicts of Interest: Authors of this manuscript declare no conflict of interest.

References

1. Jin, C.; Xiao, X.; Merbold, L.; Arneth, A.; Veenendaal, E.; Kutsch, W.L. Phenology and gross primary production of two dominant savanna woodland ecosystems in Southern Africa. *Remote Sens. Environ.* **2013**, *135*, 189–201. [CrossRef]
2. Tieszen, L.L.; Reed, B.C.; Bliss, N.B.; Wylie, B.K.; DeJong, D.D. NDVI, C3 and C4 production, and distributions in Great Plains grassland land cover classes. *Ecol. Appl.* **1997**, *7*, 59–78.
3. Polley, H.W.; Derner, J.D.; Jackson, R.B.; Wilsey, B.J.; Fay, P.A. Impacts of climate change drivers on C4 grassland productivity: Scaling driver effects through the plant community. *J. Exp. Bot.* **2014**, *65*, 3415–3424. [CrossRef] [PubMed]
4. Everson, C.S.; Everson, T. The long-term effects of fire regime on primary production of montane grasslands in South Africa. *Afr. J. Range Forage Sci.* **2016**, *33*, 33–41. [CrossRef]
5. Adair, E.C.; Burke, I.C. Plant phenology and life span influence soil pool dynamics: *Bromus tectorum* invasion of perennial C3–C4 grass communities. *Plant Soil* **2010**, *335*, 255–269. [CrossRef]
6. Adjorlolo, C.; Mutanga, O.; Cho, M.A.; Ismail, R. Challenges and opportunities in the use of remote sensing for C3 and C4 grass species discrimination and mapping. *Afr. J. Range Forage Sci.* **2012**, *29*, 47–61. [CrossRef]
7. Bremond, L.; Boom, A.; Favier, C. Neotropical C3/C4 grass distributions—Present, past and future. *Glob. Chang. Biol.* **2012**, *18*, 2324–2334. [CrossRef]
8. Chamaillé-Jammes, S.; Bond, W.J. Will global change improve grazing quality of grasslands? A call for a deeper understanding of the effects of shifts from C4 to C3 grasses for large herbivores. *Oikos* **2010**, *119*, 1857–1861. [CrossRef]
9. Winslow, J.C.; Hunt, E.R.; Piper, S.C. The influence of seasonal water availability on global C 3 versus C 4 grassland biomass and its implications for climate change research. *Ecol. Model.* **2003**, *163*, 153–173. [CrossRef]
10. White, K.; Langley, J.; Cahoon, D.; Megonigal, J.P. C3 and C4 biomass allocation responses to elevated CO_2 and nitrogen: Contrasting resource capture strategies. *Estuaries Coasts* **2012**, *35*, 1028–1035. [CrossRef]
11. Dube, T.; Mutanga, O. Evaluating the utility of the medium-spatial resolution Landsat 8 multispectral sensor in quantifying aboveground biomass in Umgeni catchment, South Africa. *ISPRS J. Photogramm. Remote Sens.* **2015**, *101*, 36–46. [CrossRef]
12. Chen, J.; Gu, S.; Shen, M.; Tang, Y.; Matsushita, B. Estimating aboveground biomass of grassland having a high canopy cover: An exploratory analysis of in situ hyperspectral data. *Int. J. Remote Sens.* **2009**, *30*, 6497–6517. [CrossRef]
13. Gao, J.-X.; Chen, Y.-M.; Lü, S.-H.; Feng, C.-Y.; Chang, X.-L.; Ye, S.-X.; Liu, J.-D. A ground spectral model for estimating biomass at the peak of the growing season in hulunbeier grassland, Inner Mongolia, China. *Int. J. Remote Sens.* **2012**, *33*, 4029–4043. [CrossRef]
14. An, N.; Price, K.P.; Blair, J.M. Estimating above-ground net primary productivity of the tallgrass prairie ecosystem of the Central Great Plains using AVHRR NDVI. *Int. J. Remote Sens.* **2013**, *34*, 3717–3735. [CrossRef]
15. Shoko, C.; Mutanga, O.; Dube, T. Progress in the remote sensing of C3 and C4 grass species aboveground biomass over time and space. *ISPRS J. Photogramm. Remote Sens.* **2016**, *120*, 13–24. [CrossRef]
16. Clevers, J.G.P.W.; Gitelson, A.A. Remote estimation of crop and grass chlorophyll and nitrogen content using red-edge bands on sentinel-2 and -3. *Int. J. Appl. Earth Obs. Geoinf.* **2013**, *23*, 344–351. [CrossRef]
17. Mutanga, O.; Skidmore, A.K. Narrow band vegetation indices overcome the saturation problem in biomass estimation. *Int. J. Remote Sens.* **2004**, *25*, 3999–4014. [CrossRef]

18. Slaton, M.R.; Hunt, E.R.; Smith, W.K. Estimating near-infrared leaf reflectance from leaf structural characteristics. *Am. J. Bot.* **2001**, *88*, 278–284. [CrossRef] [PubMed]
19. Shoko, C.; Mutanga, O. Examining the strength of the newly-launched Sentinel 2 MSI sensor in detecting and discriminating subtle differences between C3 and C4 grass species. *ISPRS J. Photogramm. Remote Sens.* **2017**, *129*, 32–40. [CrossRef]
20. Shoko, C.; Mutanga, O. Seasonal discrimination of C3 and C4 grasses functional types: An evaluation of the prospects of varying spectral configurations of new generation sensors. *Int. J. Appl. Earth Obs. Geoinf.* **2017**, *62*, 47–55. [CrossRef]
21. Nel, W. Rainfall trends in the KwaZulu-Natal Drakensberg region of South Africa during the twentieth century. *Int. J. Climatol.* **2009**, *29*, 1634–1641. [CrossRef]
22. Dollar, E.; Goudy, A. *Environmental Change: The Geography of South Africa in a Changing World*; Oxford University Press: Oxford, UK, 1999.
23. Mansour, K.; Mutanga, O.; Everson, T.; Adam, E. Discriminating indicator grass species for rangeland degradation assessment using hyperspectral data resampled to AISA eagle resolution. *ISPRS J. Photogramm. Remote Sens.* **2012**, *70*, 56–65. [CrossRef]
24. Price, K.P.; Guo, X.; Stiles, J.M. Optimal landsat TM band combinations and vegetation indices for discrimination of six grassland types in eastern Kansas. *Int. J. Remote Sens.* **2002**, *23*, 5031–5042. [CrossRef]
25. Ramoelo, A.; Cho, M.A.; Mathieu, R.; Madonsela, S.; Van De Kerchove, R.; Kaszta, Z.; Wolff, E. Monitoring grass nutrients and biomass as indicators of rangeland quality and quantity using random forest modelling and worldview-2 data. *Int. J. Appl. Earth Obs. Geoinf.* **2015**, *43*, 43–54. [CrossRef]
26. Ren, H.; Zhou, G.; Zhang, X. Estimation of green aboveground biomass of desert steppe in Inner Mongolia based on red-edge reflectance curve area method. *Biosyst. Eng.* **2011**, *109*, 385–395. [CrossRef]
27. Sibanda, M.; Mutanga, O.; Rouget, M. Examining the potential of Sentinel-2 MSI spectral resolution in quantifying above ground biomass across different fertilizer treatments. *ISPRS J. Photogramm. Remote Sens.* **2015**, *110*, 55–65. [CrossRef]
28. Sibanda, M.; Mutanga, O.; Rouget, M. Discriminating rangeland management practices using simulated hyspIRI, landsat 8 OLI, sentinel 2 MSI, and VENμs spectral data. *IEEE J. Sel. Top. Appl. Earth Obs. Remote Sens.* **2016**, *9*, 3957–3969. [CrossRef]
29. Drusch, M.; Del Bello, U.; Carlier, S.; Colin, O.; Fernandez, V.; Gascon, F.; Hoersch, B.; Isola, C.; Laberinti, P.; Martimort, P. Sentinel-2: ESA's optical high-resolution mission for GMES operational services. *Remote Sens. Environ.* **2012**, *120*, 25–36. [CrossRef]
30. Adjorlolo, C.; Mutanga, O.; Cho, M. Estimation of canopy nitrogen concentration across C3 and C4 grasslands using worldview-2 multispectral data. *Sel. Top. Appl. Earth Obs. Remote Sens.* **2014**, *7*, 4385–4392. [CrossRef]
31. Chun, H.; Keleş, S. Sparse partial least squares regression for simultaneous dimension reduction and variable selection. *J. R. Stat. Soc. Ser. B (Stat. Methodol.)* **2010**, *72*, 3–25. [CrossRef] [PubMed]
32. Sibanda, M.; Mutanga, O.; Rouget, M.; Kumar, L. Estimating biomass of native grass grown under complex management treatments using worldview-3 spectral derivatives. *Remote Sens.* **2017**, *9*, 55. [CrossRef]
33. Sibanda, M.; Mutanga, O.; Rouget, M.; Odindi, J. Exploring the potential of in situ hyperspectral data and multivariate techniques in discriminating different fertilizer treatments in grasslands. *J. Appl. Remote Sens.* **2015**, *9*, 096033. [CrossRef]
34. Abdel-Rahman, E.M.; Mutanga, O.; Odindi, J.; Adam, E.; Odindo, A.; Ismail, R. A comparison of partial least squares (PLS) and sparse PLS regressions for predicting yield of Swiss chard grown under different irrigation water sources using hyperspectral data. *Comput. Electron. Agric.* **2014**, *106*, 11–19. [CrossRef]
35. Kiala, Z.; Odindi, J.; Mutanga, O. Potential of interval partial least square regression in estimating leaf area index. *S. Afr. J. Sci.* **2017**, *113*, 1–9. [CrossRef]
36. Rigge, M.; Smart, A.; Wylie, B.; Gilmanov, T.; Johnson, P. Linking phenology and biomass productivity in south dakota mixed-grass prairie. *Rangel. Ecol. Manag.* **2013**, *66*, 579–587. [CrossRef]
37. Xie, Y.; Sha, Z.; Yu, M.; Bai, Y.; Zhang, L. A comparison of two models with landsat data for estimating above ground grassland biomass in Inner Mongolia, China. *Ecol. Model.* **2009**, *220*, 1810–1818. [CrossRef]
38. Huete, A.; Liu, H.; Batchily, K.V.; Van Leeuwen, W. A comparison of vegetation indices over a global set of TM images for EOS-MODIS. *Remote Sens. Environ.* **1997**, *59*, 440–451. [CrossRef]
39. Huete, A.R. A soil-adjusted vegetation index (SAVI). *Remote Sens. Environ.* **1988**, *25*, 295–309. [CrossRef]

40. Tucker, C.J. Red and photographic infrared linear combinations for monitoring vegetation. *Remote Sens. Environ.* **1979**, *8*, 127–150. [CrossRef]
41. Roujean, J.-L.; Breon, F.-M. Estimating par absorbed by vegetation from bidirectional reflectance measurements. *Remote Sens. Environ.* **1995**, *51*, 375–384. [CrossRef]
42. Jordan, C.F. Derivation of leaf-area index from quality of light on the forest floor. *Ecology* **1969**, *50*, 663–666. [CrossRef]
43. Addabbo, P.; Focareta, M.; Marcuccio, S.; Votto, C.; Ullo, S.L. Contribution of sentinel-2 data for applications in vegetation monitoring. *Acta IMEKO* **2016**, *5*, 44–54. [CrossRef]
44. Peterson, D.; Price, K.; Martinko, E. Discriminating between cool season and warm season grassland cover types in northeastern Kansas. *Int. J. Remote Sens.* **2002**, *23*, 5015–5030. [CrossRef]
45. Lu, S.; Shimizu, Y.; Ishii, J.; Funakoshi, S.; Washitani, I.; Omasa, K. Estimation of abundance and distribution of two moist tall grasses in the Watarase wetland, Japan, using hyperspectral imagery. *ISPRS J. Photogramm. Remote Sens.* **2009**, *64*, 674–682. [CrossRef]
46. Chen, F.; Weber, K.T.; Gokhale, B. Herbaceous biomass estimation from SPOT 5 imagery in semiarid rangelands of Idaho. *GISci. Remote Sens.* **2011**, *48*, 195–209. [CrossRef]
47. Ramoelo, A.; Skidmore, A.; Cho, M.A.; Mathieu, R.; Heitkönig, I.; Dudeni-Tlhone, N.; Schlerf, M.; Prins, H. Non-linear partial least square regression increases the estimation accuracy of grass nitrogen and phosphorus using in situ hyperspectral and environmental data. *ISPRS J. Photogramm. Remote Sens.* **2013**, *82*, 27–40. [CrossRef]
48. Delegido, J.; Verrelst, J.; Alonso, L.; Moreno, J. Evaluation of sentinel-2 red-edge bands for empirical estimation of green LAI and chlorophyll content. *Sensors* **2011**, *11*, 7063–7081. [CrossRef] [PubMed]
49. Laurin, G.V.; Puletti, N.; Hawthorne, W.; Liesenberg, V.; Corona, P.; Papale, D.; Chen, Q.; Valentini, R. Discrimination of tropical forest types, dominant species, and mapping of functional guilds by hyperspectral and simulated multispectral sentinel-2 data. *Remote Sens. Environ.* **2016**, *176*, 163–176. [CrossRef]
50. Schino, G.; Borfecchia, F.; De Cecco, L.; Dibari, C.; Iannetta, M.; Martini, S.; Pedrotti, F. Satellite estimate of grass biomass in a mountainous range in central Italy. *Agrofor. Syst.* **2003**, *59*, 157–162. [CrossRef]
51. Sharma, L.K.; Bu, H.; Denton, A.; Franzen, D.W. Active-optical sensors using red NDVI compared to red edge NDVI for prediction of corn grain yield in North Dakota, USA. *Sensors* **2015**, *15*, 27832–27853. [CrossRef] [PubMed]
52. Grant, K.M.; Johnson, D.L.; Hildebrand, D.V.; Peddle, D.R. Quantifying biomass production on rangeland in southern Alberta using SPOT imagery. *Can. J. Remote Sens.* **2013**, *38*, 695–708. [CrossRef]
53. Guan, L.; Liu, L.; Peng, D.; Hu, Y.; Jiao, Q.; Liu, L. Monitoring the distribution of C3 and C4 grasses in a temperate grassland in Northern China using moderate resolution imaging spectroradiometer normalized difference vegetation index trajectories. *J. Appl. Remote Sens.* **2012**, *6*, 063535.
54. Pau, S.; Still, C.J. Phenology and productivity of C3 and C4 grasslands in Hawaii. *PLoS ONE* **2014**, *9*, e107396. [CrossRef] [PubMed]
55. Davidson, A.; Csillag, F. The influence of vegetation index and spatial resolution on a two-date remote sensing-derived relation to C4 species coverage. *Remote Sens. Environ.* **2001**, *75*, 138–151. [CrossRef]
56. Ediriweera, S.; Pathirana, S.; Danaher, T.; Nichols, D. Estimating above-ground biomass by fusion of LiDAR and multispectral data in subtropical woody plant communities in topographically complex terrain in north-eastern Australia. *J. For. Res.* **2014**, *25*, 761–771. [CrossRef]
57. Man, Q.; Dong, P.; Guo, H.; Liu, G.; Shi, R. Light detection and ranging and hyperspectral data for estimation of forest biomass: A review. *J. Appl. Remote Sens.* **2014**, *8*, 081598. [CrossRef]
58. Epstein, H.; Lauenroth, W.; Burke, I.; Coffin, D. Productivity patterns of C3 and C4 functional types in the US great plains. *Ecology* **1997**, *78*, 722–731.